Thermochimica Acta, 60 (1983) 361–381
Elsevier Scientific Publishing Company, Amsterdam – Printed in The Netherlands

THERMAL DECOMPOSITION OF MAGNESIAN KUTNAHORITE

K. IWAFUCHI, C. WATANABE and R. OTSUKA
Department of Mineral Industry, Waseda University, Tokyo (Japan)

(Received 30 June 1982)

ABSTRACT

This work investigates the thermal decomposition of magnesian kutnahorite, which belongs to the dolomite group.

The DTA curve measured in static air using a small amount of sample (5.0 mg) is quite different from those published previously. This difference might be due to the effect of a self-generated CO_2 atmosphere.

In a CO_2 flow of 100 ml min^{-1}, magnesian kutnahorite decomposes in four steps.

$$\begin{aligned}\text{Mg-kutnahorite} &\rightarrow CaCO_3 + Mg_2MnO_4 + Mn_3O_4 + MgO \\ &\rightarrow CaCO_3 + CaMnO_3 + MgO \\ &\rightarrow CaCO_3 + CaMnO_3 + Ca_2MnO_4 + MgO \\ &\rightarrow CaMnO_3 + Ca_2MnO_4 + MgO + CaO.\end{aligned}$$

However, in a mixed gas flow of CO_2 at 95 ml min^{-1} and CO at 5 ml min^{-1}, it decomposes, like dolomite, in two steps.

$$\begin{aligned}\text{Mg-kutnahorite} &\rightarrow CaCO_3 + (Mg,Mn)\underline{O} \\ &\rightarrow (Ca,Mn)O + (Mg,Mn)\overline{O}.\end{aligned}$$

It has been found that the equilibrium redistribution of Mn between (Ca, Mn)O and (Mg, Mn)$\overline{O}$ is achieved at the second decomposition step. This is supported by theoretical considerations.

Consequently, when the O_2 partial pressure in the atmosphere is low enough to keep Mn in a bivalent state, the Mn bearing dolomite group mineral decomposes in a similar manner to dolomite itself.

INTRODUCTION

The dolomite group includes dolomite, $CaMg(CO_3)_2$, ankerite, $CaFe(CO_3)_2$, and kutnahorite, $CaMn(CO_3)_2$. Of the minerals in this group, dolomite is the most common, ankerite less common and kutnahorite is of rare occurrence. The name kutnahorite was first proposed by Bukowsky for a supposed member of the dolomite group, ideally $CaMn(CO_3)_2$ (Frondel and Bauer [1]). Later, based on their mineralogical investigation on the carbonate minerals from Kutna Hora, Czechoslovakia, and Franklin and

0040-6031/83/0000–0000/$03.00

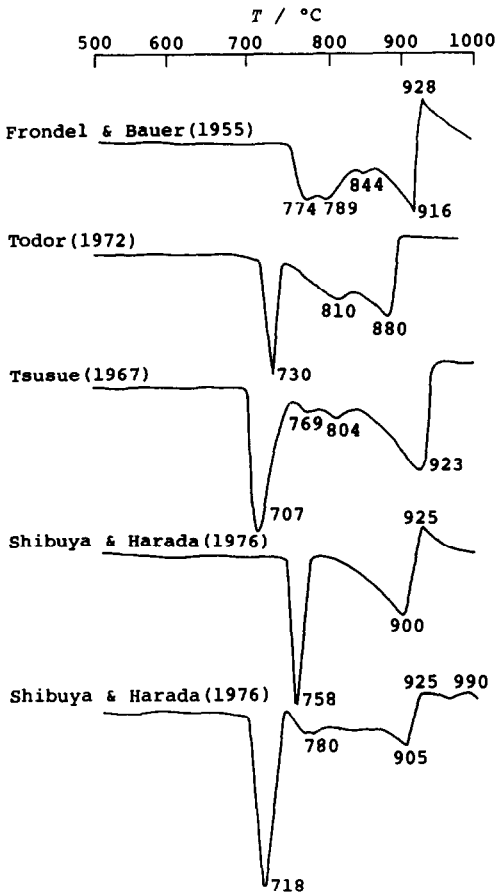

Fig. 1. Some DTA curves of kutnahorite published previously.

Stering Hill, New Jersey, U.S.A., Frondel and Bauer [1] established the existence of kutnahorite as a valid member of the dolomite group.

DTA curves of kutnahorite were presented by several workers, e.g. Frondel and Bauer [1], Todor [2], Tsusue [3] and Shibuya and Harada [4] (Fig. 1). However, analysis of the curves was performed only by Shibuya and Harada [4]. In addition, the DTA curves hitherto presented were measured for rather large amounts of samples and in static air atmospheres. Under these conditions, the detailed interpretation of the results would be difficult.

In this study, as a part of the thermoanalytical investigation of dolomite and related minerals by Otsuka et al. [5,6], kutnahorite was selected in order to examine how substituent Mn^{2+} in the dolomite structure affects the thermal decomposition of dolomite itself. The investigation was performed by means of DTA for small amounts of samples in flowing gas atmospheres and by the X-ray powder method.

MATERIAL

Magnesian kutnahorite from the Ryujima mine, Nagano Prefecture, Japan was used in this study, since its mineralogical properties were reported in detail by Tsusue [3]. It was found that the Fe content in this mineral was very low compared with Mn.

The present material is coarse granular with perfect cleavage on r, {104} (indexed based on the true structural cell). It is white to pale pink with a vitreous to pearly lustre. Streaks are white to pale pink. It is brittle and has a Mohs hardness of 3.5–4.

Samples were prepared by handpicking under a binocular microscope.

Chemical composition (wt.%) and cation mole ratio (mole %) of the sample were obtained by electron probe microanalysis (EPMA) (apparatus, JEOL JXA-50A). Correction was made by the method of Bence and Albee (Table 1). The structural formula was calculated assuming oxygen number as 6: $Ca_{1.064}(Mn_{0.475}Mg_{0.437}Fe_{0.024})(CO_3)_2$.

X-Ray powder analysis confirmed that this material was free from other minerals. Lattice parameters, using silicon (99.9999%) as an internal standard were found to be $a = 4.8429 \pm 0.0003$ Å and $c = 16.195 \pm 0.001$ Å.

The ordered reflections (003) and (015) observed in the powder pattern (Fig. 2) show that this material belongs to the dolomite group of $R\bar{3}$ symmetry.

Magnesian kutnahorite is abbreviated to Mg-kutnahorite in this paper.

EXPERIMENTAL

Mg-kutnahorite was ground in an agate mortar and fractions finer than 325 mesh (43 μm) for experiment were obtained by sieving.

TABLE 1

Chemical composition (weight %) and cation mole ratio (mole %) of Mg-kutnahorite

	Wt.%		Cation mole ratio (mole %)
CaO	28.6	$CaCO_3$	53.20
MgO	8.4	$MgCO_3$	21.83
FeO	0.8	$FeCO_3$	1.22
MnO	16.1	$MnCO_3$	23.75
CO_2	42.1		
Total	96.0		

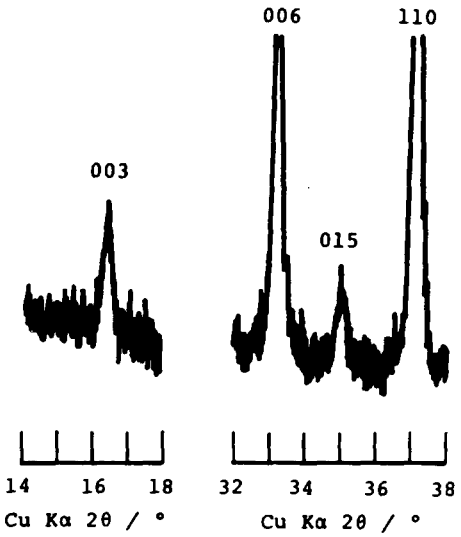

Fig. 2. The ordered reflections of Mg-kutnahorite showing dolomite-like structure.

DTA measurement

DTA curves were recorded by a Shinku Riko ULVAC DT-1500H incorporating a Pt–PtRh 13% thermocouple, Pt micro sample pan and calcined alumina as a reference material, under the conditions: sample weight 5.0 mg, programmed heating rate 10°C min^{-1}, DTA sensitivity $\pm$ 50 μV. Measurements were performed in (a) static air, (b) CO_2 flow at 100 ml min^{-1}, and (c) a mixed gas flow of CO_2 at 95 ml min^{-1} and CO at 5 ml min^{-1}. In the following discussion, these atmospheres are abbreviated as air, CO_2 and CO_2 + CO, respectively.

X-Ray powder analysis

The phase identification of the reaction products was made by X-ray powder analysis with a Rigaku Geigerflex 2001, under the following conditions; Ni-filtered CuK_α radiation ($\lambda = 1.5418$ Å), 40 kV, 20 mA, time constant 2 s, scanning speed 0.5° min^{-1}, divergence slit 1°, receiving slit 0.3 mm and scattering slit 1°.

After being heated to certain temperatures (determined by the DTA curves), the samples were rapidly cooled down to room temperature by removing the furnace, and then subjected to X-ray analysis.

RESULTS

DTA curves

Figure 3 shows the DTA curves of Mg-kutnahorite in the three atmospheres.

The DTA curve obtained in air (A) has a broad and asymmetric endotherm followd by a step-like shoulder. This is remarkably different from those in Fig. 1.

The DTA curve obtained in CO_2 (B) shows four discrete endothermic peaks as well as a very weak exothermic hump immediately after the first one. The second and third peaks are fairly broad, despite their low peak heights, showing characteristic symmetric shape like an isosceles triangle.

The DTA curve obtained in $CO_2 + CO$ (C) shows two endothermic peaks similar to that of dolomite in CO_2, though the peak temperatures of Mg-kutnahorite are lowered.

Identification of products

Since it was considered from the discrete endothermic peaks that each step of the decomposition could be examined separately, the products in

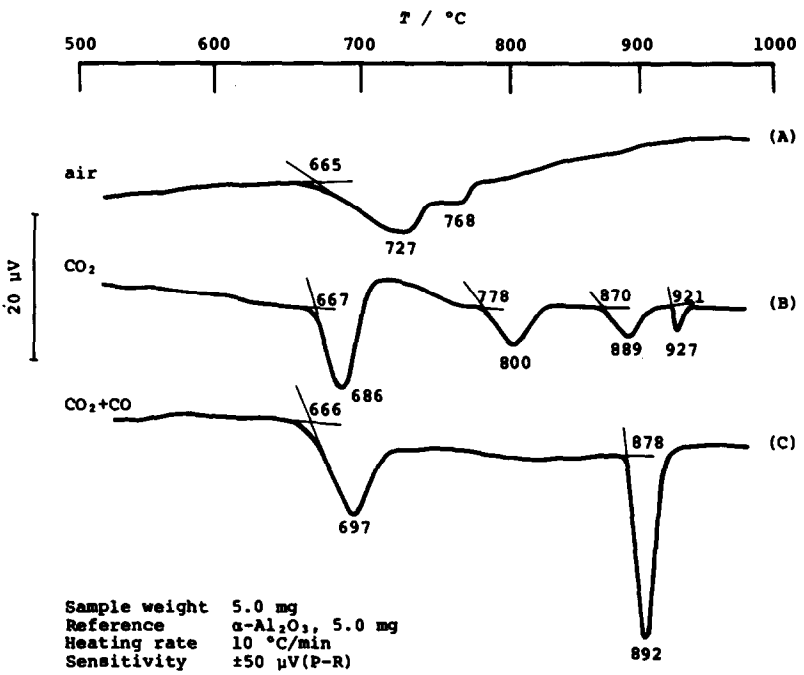

Fig. 3. DTA curves of Mg-kutnahorite under the three atmospheres.

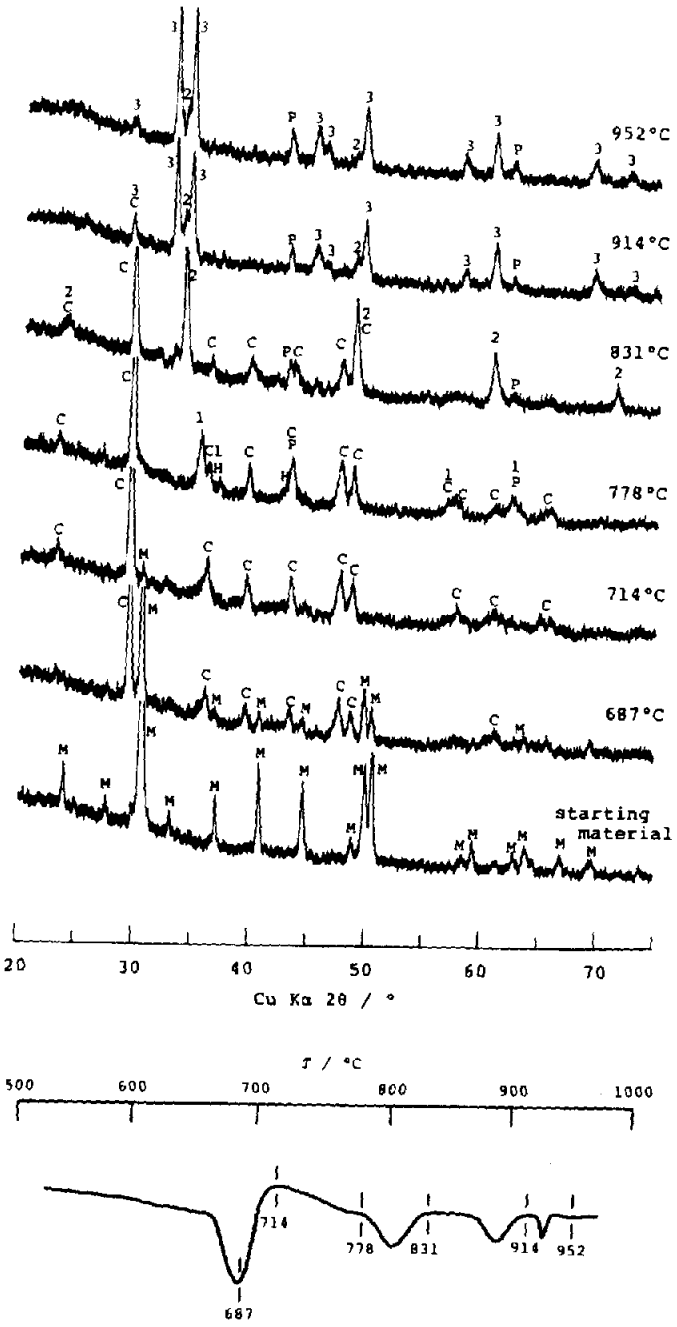

Fig. 4. X-Ray diffraction patterns of thermal decomposition products of Mg-kutnahorite in CO_2. M, Mg-kutnahorite; C, $CaCO_3$; P, MgO; H, Mn_3O_4; 1, Mg_2MnO_4; 2, $CaMnO_3$; 3, Ca_2MnO_4. Each temperature to which the sample was heated is indicated beneath the DTA curve in the lower part.

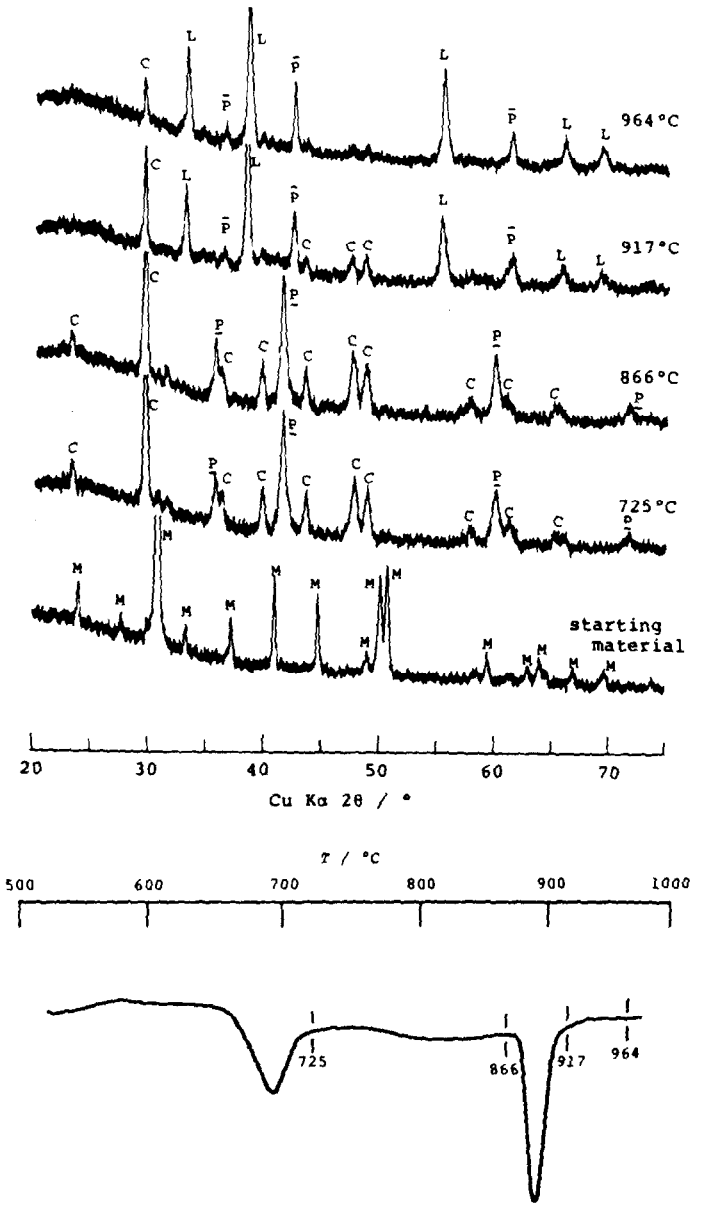

Fig. 5. X-Ray diffraction patterns of thermal decomposition products of Mg-kutnahorite in $CO_2 + CO$. M, Mg-kutnahorite; C, $CaCO_3$; P, (Mg, Mn)O; $\bar{P}$, (Mg, Mn)O; L, (Ca, Mn)O. Each temperature to which the sample was heated is indicated beneath the DTA curve in the lower part.

CO_2 and CO_2 + CO were observed by X-ray powder analysis. These results are shown in Figs. 4 and 5. Each temperature, to which the sample was heated, is indicated beneath the DTA curves in the lower parts of both figures. The X-ray powder patterns of the products obtained by heating are

TABLE 2

Thermal decomposition products of Mg-kutnahorite in CO_2

Temperature, T (°C)	Products observed by powder X-ray method
687	$CaCO_3$, Mg-kutnahorite
714	$CaCO_3$, Mg-kutnahorite
778	$CaCO_3$, Mg_2MnO_4, Mn_3O_4, MgO
831	$CaMnO_3$, $CaCO_3$, MgO
914	Ca_2MnO_4, $CaMnO_3$, MgO $CaCO_3$
952	Ca_2MnO_4, $CaMnO_3$, MgO, $CaCO_3$

reproduced in the upper parts. The products identified are listed in Tables 2 and 3.

In CO_2 (Fig. 4), at 687 and 714°C, only $CaCO_3$ was observed clearly and any products containing Mn and/or Mg could hardly be detected. At 778°C, Mg_2MnO_4, MgO and Mn_3O_4 as well as $CaCO_3$ were found. However, many reflections of these three products overlapped and, moreover, MgO and Mn_3O_4 had very weak reflections, so that the precise identification of the products was very difficult. At 831°C, with the decrease of the amount of $CaCO_3$, Mg_2MnO_4 and Mn_3O_4 disappeared completely, while $CaMnO_3$ and MgO were found. At 914°C, a new phase Ca_2MnO_4 appeared together with small amounts of $CaCO_3$ and $CaMnO_3$. At 952°C, almost all the $CaCO_3$ disappeared, though the reflections of the other products became more intense. The cooling DTA curve, recorded at a programmed rate of 10°C min^{-1} after the completion of the decomposition, showed that only the fourth peak gave a reverse exothermic peak. This confirmed that the fourth peak was due to the decomposition of $CaCO_3$.

In $CO_2 + CO$ (Fig. 5), at 725°C, $CaCO_3$ and periclase solid solution (Mg, Mn)$\underline{O}$ were observed. At 917°C, lime solid solution (Ca, Mn)O and periclase solid solution (Mg, Mn)$\overline{O}$ as well as a trace amount of $CaCO_3$ appeared. The periclase solid solution decreased its lattice parameter from (Mg, Mn)$\underline{O}$ to (Mg, Mn)$\overline{O}$.

TABLE 3

Thermal decomposition products of Mg-kutnahorite in $CO_2 + CO$

Temperature, T (°C)	Products observed by powder X-ray method
725	$CaCO_3$, (Mg, Mn)$\underline{O}$
866	$CaCO_3$, (Mg, Mn)$\underline{O}$
917	(Ca, Mn)O, (Mg, Mn)$\overline{O}$, $CaCO_3$
964	(Ca, Mn)O, (Mg, Mn)$\overline{O}$, $CaCO_3$

DISCUSSION

DTA curve in air

The DTA curve measured in air [Fig. 3(A)] is different from any curves in previous works [1–4] (Fig. 1). It is especially noteworthy that although the curve by Tsusue [3] was obtained on magnesian kutnahorite from the same locality as the sample in this study, both results differ greatly in peak shapes and peak temperature ranges.

The authors observed previously [5] the variation in the DTA curves of dolomite under different measurement conditions. Figure 6 shows that a small amount of sample (5.0 mg) gives a single endothermic peak (A), while a larger amount of sample (100 mg) gives two separate endothermic peaks (B). This phenomenon may be due to the effect of the self-generated CO_2, produced and accumulated around and in the sample with the progress of the decomposition.

In this way, the marked difference between the DTA curves by the present

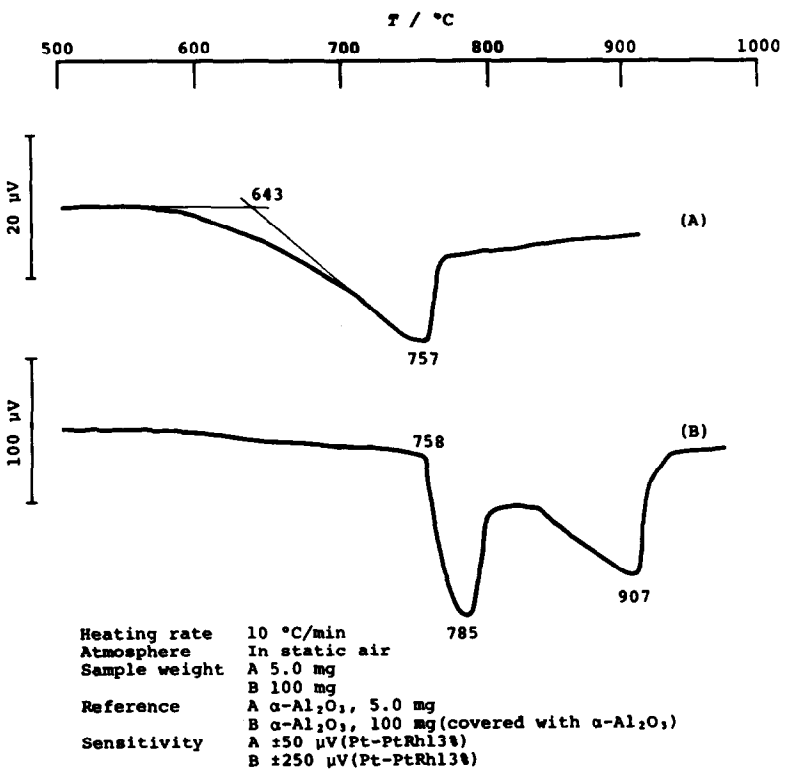

Fig. 6. Variation of DTA curves of dolomite due to the effect of the self-generated CO_2 atmosphere.

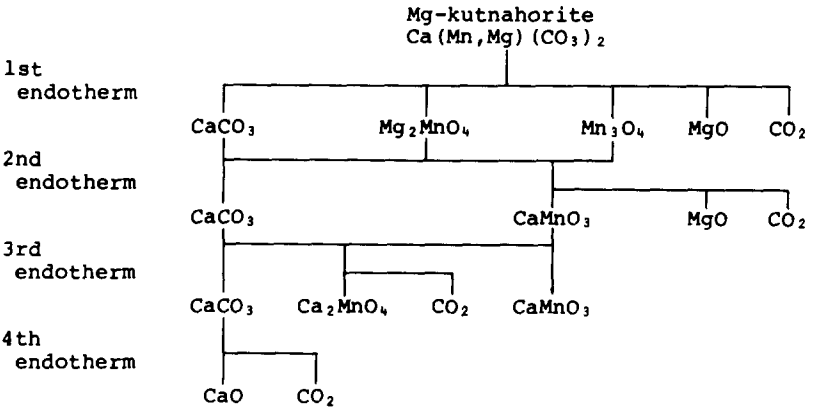

Fig. 7. Thermal decomposition process of Mg-kutnahorite in CO_2.

authors and other workers, especially Tsusue [3], may be ascribed to the different effects of the self-generated CO_2 determined by a wide variety of sample amounts and sample holders.

The DTA curve of Mg-kutnahorite in air indicates that the decomposition of this mineral proceeds not in a single step, but in some parallel processes. The analysis of the results is complicated by these simultaneous reactions, so it is omitted in this study.

Decomposition in CO_2

Mg-kutnahorite decomposes in four steps in CO_2 as indicated in Fig. 7. At the first step, the original Mg-kutnahorite decomposes into $CaCO_3$, Mg_2MnO_4, Mn_3O_4 and MgO with the release of CO_2 of the corresponding amount to Mn and Mg. At the second step, Mg_2MnO_4 and Mn_3O_4 react with part of the $CaCO_3$ to produce $CaMnO_3$ and MgO. At the third step, $CaMnO_3$ reacts with the remaining $CaCO_3$, and Ca_2MnO_4 is formed. In this step, a small amount of $CaMnO_3$ remains though enough $CaCO_3$ to be reacted still exists. This would be due to insufficient contact between solid particles. At the fourth step, as confirmed by the reverse exothermic peak on cooling, the residual $CaCO_3$ decomposes.

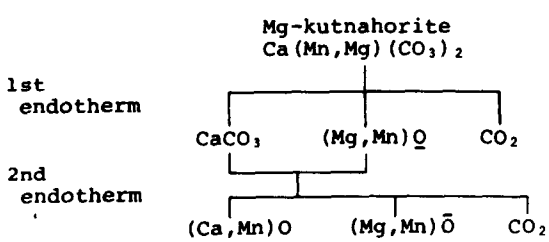

Fig. 8. Thermal decomposition process of Mg-kutnahorite in $CO_2 + CO$.

Shibuya and Harada [4] showed the reaction processes

$$CaMn(CO_3)_2 \rightarrow CaCO_3 + CaMnO_3 \rightarrow Ca_4Mn_3O_{10} + CaMn_2O_4 + CaMnO_3$$

$$Ca(Mn,Mg)(CO_3)_2 \rightarrow CaCO_3 + CaMnO_3 + MgO \rightarrow CaMn_2O_4 + CaMnO_3 + MgO + CaO$$

for the decomposition of kutnahorite and magnesian kutnahorite in air. They identified $Ca_4Mn_3O_{10}$ as a decomposition product of kutnahorite, but they did not observe the same material in the products of magnesian kutnahorite having a greater Ca/Mn ratio than kutnahorite. This unreasonable observation could be avoided if $CaMn_2O_4$ was replaced by Ca_2MnO_4 and the excess Ca assigned to this phase. Then, the reflection ($d = 2.600$–2.615 Å), which remained unidentified by Shibuya and Harada [4], could be assigned as the second strongest peak of Ca_2MnO_4, and the above decomposition process of magnesian kutnahorite could be rewritten

$$Ca(Mn,Mg)(CO_3)_2 \rightarrow CaCO_3 + CaMnO_3 + MgO \rightarrow Ca_2MnO_4 + CaMnO_3 + MgO + CaO$$

These products are the same as those obtained at the second and fourth steps in this study.

Tanida et al. [7] observed Ca_2MnO_4 as a decomposition product of calcian kutnahorite having a Ca/Mn ratio of about 2 in air.

These results show that Ca_2MnO_4 is a rather common decomposition product of kutnahorite in which the Ca/Mn ratio is equal to about 2, though this material is not found in the phase diagram of the Ca–Mn-oxide system constructed by Riboud and Muan [8], as suggested by Tanida et al. [7].

Decomposition in CO_2 + CO

Figure 8 shows the decomposition process of Mg-kutnahorite in CO_2 + CO. In this atmosphere, Mg-kutnahorite decomposes in two steps like dolomite in CO_2.

At the first step, the original Mg-kutnahorite decomposes into $CaCO_3$ and periclase solid solution (Mg,Mn)$\underline{O}$, and releasing CO_2 of the corresponding amount to Mn and Mg. At the second step, (Mg,Mn)$\underline{O}$ reacts with $CaCO_3$ to produce lime solid solution (Ca, Mn)O and periclase solid solution (Mg, Mn)$\overline{O}$. Owing to the re-distribution of Mn between (Mg, Mn)$\underline{O}$ and CaO produced from $CaCO_3$ at this step, the lattice parameters of (Ca, Mn)O and (Mg, Mn)$\overline{O}$ become smaller than those of CaO and (Mg, Mn)$\underline{O}$.

The lattice parameter of each solid solution before and after the second peak is determined using its (200) reflection

(Mg,Mn)$\underline{O}$ $a = 4.3515$ Å

(Mg,Mn)$\overline{O}$ $a = 4.2086$ Å

(Ca,Mn)O $a = 4.7028$ Å

As the CaO–MgO system scarcely forms solid solution series below 1000°C [9], (Ca, Mg)O and (Ca, Mg, Mn)O are not considered in the following discussion.

From the relation between chemical composition and lattice parameter in the CaO–MnO and MgO–MnO systems determined by Jay and Andrews [10], the chemical composition of each of the above solid solutions can be estimated

$$(Mg,Mn)\underline{O} \quad (Mg_{0.454} \quad Mn_{0.546})O$$
$$(Mg,Mn)\overline{O} \quad (Mg_{0.784} \quad Mn_{0.216})O$$
$$(Ca,Mn)O \quad (Ca_{0.700} \quad Mn_{0.300})O$$

Since the estimated Mg/Mn ratio (45.4/54.6) of (Mg, Mn)$\underline{O}$ agrees with that (47.89/52.11) of the original Mg-kutnahorite obtained by EPMA, all the Mn in Mg-kutnahorite is considered to have been incorporated into (Mg, Mn)$\underline{O}$ at the first step. Thus, the chemical composition of (Mg, Mn)$\underline{O}$ will be represented as $(Mg_{21.83}Mn_{26.25})O_{48.08}$, based on the $MgCO_3$ mole % of 21.83 in Mg-kutnahorite as given in Table 1. Although the Mn content of 26.25, estimated by the lattice parameter, is slightly different from that of 23.75 obtained by EPMA, the former content is used here, considering the error to be of this extent. Further, the Fe content is found to be less than 5% of the Mn content, hence Fe may be ignored throughout the following discussion.

In the formation of the above solid solutions, all the Mg and Mn is considered to have participated. However, in the case of Ca, the amount which participated is unknown, because it was clearly ascertained that a part of Ca was eliminated as recombined $CaCO_3$ on cooling, so it has been estimated as follows.

The chemical composition of (Mg, Mn)$\overline{O}$ estimated by the lattice parameter can be represented as $(Mg_{21.83}Mn_{6.01})O_{27.84}$ on the basis of the Mg content of 21.83 provided all the Mg is contained in it. Thus, leaving 6.01 in (Mg, Mn)$\overline{O}$, the remaining Mn of 20.24 will migrate into (Ca, Mn)O. Hence, the chemical composition of (Ca, Mn)O will be represented as $(Ca_{47.23}Mn_{20.24})O_{67.47}$ on the basis of the Mn content of 20.24. Consequently, the amount of Ca which participates in the formation of (Ca, Mn)O will equal 47.23, and it reaches about 90% of the total amount in the original Mg-kutnahorite.

The equilibrium distribution of Mn between the periclase and lime solid solutions can be expressed by the Nernst distribution law

$$\mu^{P}_{MnO} = \mu^{L}_{MnO} \tag{1}$$

where P and L represent the periclase and lime phases. In this case, the above condition is simply expressed by the activity of the MnO component

in both phases

$$a^{P}_{MnO} = a^{L}_{MnO} \tag{2}$$

When the MnO content in (Mg, Mn)$\overline{O}$ and in (Ca, Mn)O is expressed by u and v, respectively, the total amount of Mn can be represented by

$$u + v = 26.25 \tag{3}$$

The mole fraction of MnO in (Mg, Mn)$\overline{O}$, x^{P}_{MnO}, and that in (Ca, Mn)O, x^{L}_{MnO}, is expressed by

$$x^{P}_{MnO} = \frac{u}{(21.83 + u)} \tag{4}$$

$$x^{L}_{MnO} = \frac{v}{(47.23 + v)} = \frac{(26.25 - u)}{(73.48 - u)} \tag{5}$$

The activity of the MnO component in both phases was estimated from the relation between activity and mole fraction of the MgO–MnO system (Hahn and Muan [11]) and of the CaO–MnO system (Tiberg and Muan [12]) at 1100°C, because available data for the temperature region of this experiment (500–1000°C) are lacking.

Figure 9 shows the activity of the MnO component in both phases at various u values. The intersection gives the Mn contents at which the MnO component has the same activity value in both phases.

The value of $u = 6.02$ at the intersection agrees very well with the Mn content of 6.01 in (Mg, Mn)$\overline{O}$ obtained by the lattice parameter. This agreement suggests that equilibrium redistribution of Mn between (Mg, Mn)$\overline{O}$ and (Ca, Mn)O is achieved at the second step of the decomposition and that the Mn may migrate fast enough to reach the equilibrium state.

Although all the Mn has been assumed to be contained in (Mg, Mn)$\underline{O}$ in

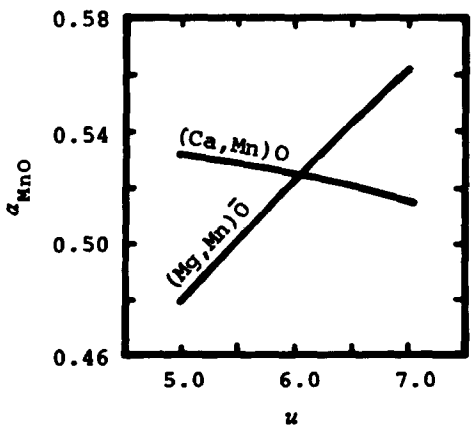

Fig. 9. Activity of MnO component in (Mg, Mn)$\overline{O}$ and (Ca, Mn)O vs. MnO content (u) in (Mg, Mn)$\overline{O}$.

the foregoing discussion, it may be possible to consider that at the first step, equilibrium distribution of Mn between the two products, $CaCO_3$ and (Mg, Mn)O, is achieved. On this assumption, Mn migration at the first step may be expressed as

$$MnCO_3[\text{component in } CaCO_3] = MnO[\text{component in (Mg,Mn)O}] + CO_2$$

The equilibrium state of this reaction can be represented

$$\Delta G_r^0 = -RT \ln K \tag{6}$$

$$\Delta G_r^0 = \mu_{MnO}^0 + \mu_{CO_2}^0 - \mu_{MnCO_3}^0 \tag{7}$$

$$K = \frac{a_{MnO}^{P} P_{CO_2}}{a_{MnCO_3}^{C}} \tag{8}$$

where P and C represent periclase and calcite phases and ^{0} denotes the thermodynamic standard state.

At the temperatures before and after the first peak, the equilibrium constant K is estimated using the available thermodynamic data (Robie and Waldbaum [13])

at 900 K (626.85°C) $K = 299.82$

at 1000 K (726.85°C) $K = 1203.64$

As the Gibbs energy of formation of $MnCO_3$ is given only up to 700 K, the values at higher temperatures are estimated by the extrapolation of the free energy function. P_{CO_2} is evaluated as 0.95 atm under the mixing condition in CO_2 + CO atmosphere. The activity of the MnO component in (Mg, Mn)O, a_{MnO}^{P}, was approximated as 0.8 from the relation between activity and mole fraction of the MgO–MnO system at 1100°C (Hahn and Muan [11]), since there is no available data for the temperature region of this experiment (500–1000°C).

Substituting $P_{CO_2} = 0.95$ atm and $a_{MnO}^{P} = 0.8$ into eqn. (8), the activity of the $MnCO_3$ component in $CaCO_3$, $a_{MnCO_3}^{C}$, can be evaluated at 900 and 1000 K, where K was estimated previously

at 900 K (626.85°C) $a_{MnCO_3}^{C} = 2.5 \times 10^{-3}$

at 1000 K (726.85°C) $a_{MnCO_3}^{C} = 6.3 \times 10^{-4}$

These are very small compared with a_{MnO}^{P}. As there is no available data for the relation between activity and mole fraction in the $CaCO_3$–$MnCO_3$ system, the mole fraction cannot be estimated from the above activity directly. However, if this system reveals positive deviation from the behaviour of an ideal solution such as the CaO–MnO system (Tiberg and Muan [12]) the mole fraction may be less than the corresponding activity. Accordingly, the assumption that all the Mn is contained in (Mg, Mn)O at the first step decomposition may hold safely. After all, if Mn is supposed to

behave like Mg, the first step decomposition of Mg-kutnahorite will proceed similarly to that of dolomite

$Ca(Mn,Mg)(CO_3)_2 \rightarrow CaCO_3 + (Mg,Mn)\underline{O} + CO_2$ (Mg-kutnahorite)

$CaMg(CO_3)_2 \rightarrow CaCO_3 + MgO + CO_2$ (dolomite)

Regarding the second step decomposition, Mg-kutnahorite is more complicated than dolomite due to the redistribution of Mn between the products. However, since the release of CO_2 from $CaCO_3$ may be regarded as the main reaction, this decomposition of Mg-kutnahorite corresponds well to that of dolomite. In other words, since its products scarcely form a solid solution through decomposition, the decomposition of dolomite may be the most simple reaction in the dolomite group.

O_2 partial pressures of the atmospheres in the experiments

According to the foregoing results of the decomposition of Mg-kutnahorite, Mn remains bivalent in $CO_2 + CO$, while in CO_2, it is finally oxidized to tetravalent Mn. This difference in the valence of Mn causes the difference in the decomposition process of this mineral and the products formed. Therefore, it will be very important to investigate the effect of O_2 partial pressure

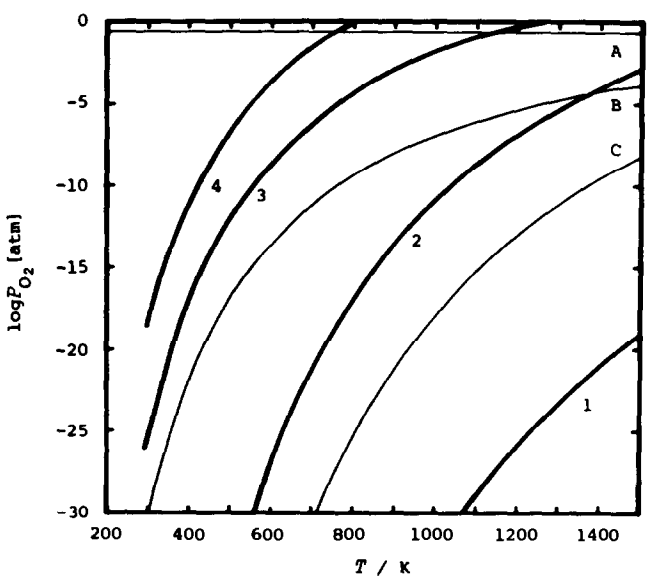

Fig. 10. Equilibrium O_2 partial pressure vs. temperature in the system Mn-O under 1 atm total pressure.
1, 2 MnO = 2 Mn + O_2
2, 2 Mn_3O_4 = 6 MnO + O_2
3, 6 Mn_2O_3 = 4 Mn_3O_4 + O_2
4, 4 MnO_2 = 2 Mn_2O_3 + O_2
A, P_{O_2} in air; B, P_{O_2} in CO_2; and C, P_{O_2} in CO_2 + CO.

on the thermal decomposition of carbonates containing transition metal elements.

Accordingly, the oxidation state of Mn in the same atmospheres as in this study was examined using $MnCO_3$ (rhodochrosite) as a test sample. As a result, Mn_3O_4 was observed in CO_2 and MnO in $CO_2 + CO$ as the decomposition products of $MnCO_3$.

Figure 10 shows the equilibrium O_2 partial pressure curves at various temperatures in the Mn–O system under 1 atm total pressure. The equilibrium O_2 partial pressures in CO_2 and $CO_2 + CO$, which were determined by dissociation of CO_2 into CO and O_2, are also shown in Fig. 10. These were estimated as follows.

The basic dissociation reaction is

$$2\,CO_2 = 2\,CO + O_2$$

In the present experiments, the flow rates of CO_2 and CO were adjusted so as to keep the amount of total flow at 100 ml min^{-1}, and this mixing gas was introduced into the reaction chamber. This condition may be approximated by the initial condition that pure CO_2 at $P^i_{CO_2}$ atm and pure CO at P^i_{CO} atm are mixed at the condition of

$$P^i_{CO_2} + P^i_{CO} = 1 \text{ atm} \tag{9}$$

If the dissociation equilibrium is achieved quickly in the reaction chamber, the condition that the flowing gas is released into the open air may be expressed as

$$P_{CO_2} + P_{CO} + P_{O_2} = 1 \text{ atm} \tag{10}$$

where P_{CO_2}, P_{CO} and P_{O_2} are the equilibrium partial pressures (atm), respectively.

The equilibrium condition expressed by

$$\Delta G^0_r = -RT \ln K \tag{11}$$

$$\Delta G^0_r = 2\,\mu^0_{CO} + \mu^0_{O_2} - 2\,\mu^0_{CO_2} \tag{12}$$

$$K = \frac{P^2_{CO} P_{O_2}}{P^2_{CO_2}} \tag{13}$$

From the balance of carbon and oxygen before and after the equilibrium, the equation

$$\frac{2P^i_{CO_2} + P^i_{CO}}{P^i_{CO_2} + P^i_{CO}} = \frac{2P_{CO_2} + P_{CO} + 2P_{O_2}}{P_{CO_2} + P_{CO}} \tag{14}$$

is constructed.

An algebraic equation of P_{O_2}, derived from eqns. (9)–(14), is solved by the Newton–Raphson method using appropriate thermodynamic data (Robie

and Waldbaum [13]) under the initial conditions $P^{i}_{CO_2} = 1$ atm and $P^{i}_{CO} = 0$ atm in CO_2, and $P^{i}_{CO_2} = 0.95$ atm and $P^{i}_{CO} = 0.05$ atm in $CO_2 + CO$.

In Fig. 10, the O_2 partial pressure curve in CO_2 (B) is above the $MnO-Mn_3O_4$ equilibrium curve (2) in the experimental range 800–1300 K, therefore the formation of Mn_3O_4 may be favoured in CO_2. However, the O_2 partial pressure curve in $CO_2 + CO$ (C) is in the MnO stability region which is bounded by the equilibrium curves of Mn–MnO (1) and $MnO-Mn_3O_4$ (2), therefore the formation of MnO may be preferred in $CO_2 + CO$.

These estimations can elucidate well the results of the decomposition of $MnCO_3$ under both atmospheres. Therefore, it is inferred that the estimated O_2 partial pressure is attained in the DTA reaction chamber used in this study.

Accordingly, in the $CO_2 + CO$ atmosphere, since it exists stably as a bivalent cation, Mn can form a solid solution with MgO. This is the most important condition at which Mg-kutnahorite decomposes in two steps like dolomite.

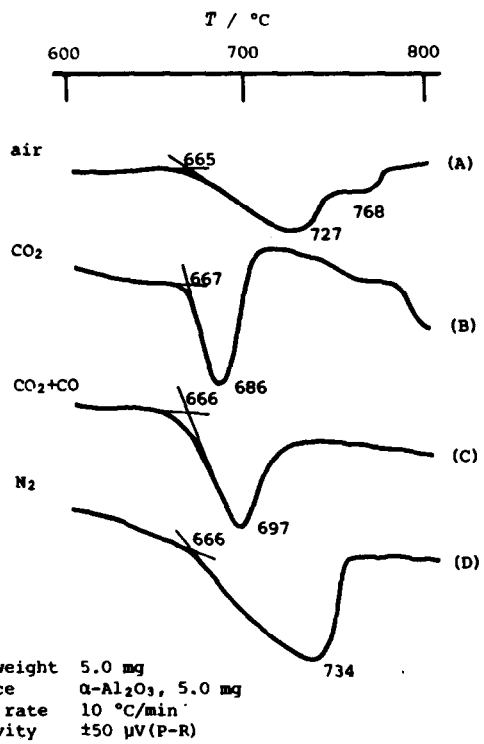

Fig. 11. The extrapolated onset temperatures ($T_{e.o.}$) of the first endothermic peaks under various atmospheres.

Agreement of the extrapolated onset temperatures of the first endothermic peaks in various atmospheres

Figure 11 shows the DTA curves between 600 and 800°C obtained in air (A), in CO_2 (B) and in $CO_2 + CO$ (C). Although CO_2 and O_2 partial pressures are remarkably different among these atmospheres, the extrapolated onset temperatures of the first peak ($T_{e.o.}$) agree very well with each other, i.e. 665°C in air, 667°C in CO_2 and 666°C in $CO_2 + CO$. The curve (D) obtained in flowing N_2 at 100 ml min^{-1} also shows the identical $T_{e.o.}$ of 666°C (Fig. 11).

In order to interpret this result, the reaction mechanism proposed by Haul and Heystek [14] to explain the two step decomposition of dolomite may be useful. They observed that the peak temperature of the first endotherm of dolomite was independent of the CO_2 partial pressure in the atmosphere, and proposed that this reaction was preceded by the mutual diffusion of the component cations within the lattice. The result observed in this study may also be interpreted similarly. Independent of the atmospheres, when Mg-kutnahorite is heated up to a certain temperature (in this case, 666°C), Ca and (Mg, Mn) cations obtain enough energy to migrate to the counter directions and form Ca-rich and (Mg, Mn)-rich regions. As the latter is unstable at such a temperature, it decomposes immediately releasing CO_2.

The good agreement of the $T_{e.o.}$ of the first endotherms probably suggests that, the same mechanism mentioned above governs the reaction through the initial decomposition period until the original structure is destroyed. However, after the destruction of the original structure, Mg-kutnahorite decomposes in quite different ways depending on the oxidation state of Mn which is changed easily by the atmosphere.

Consequently, it is suggested that in Mg-kutnahorite the cation diffusion mechanism, which is activated only by heating up to a characteristic temperature, is more significant than in dolomite. In the case of dolomite, the value of $T_{e.o.}$ of the first endotherm is lowered in air and in N_2, and such a consistency as was found in Mg-kutnahorite is not recognized. Moreover, Bandi and Krapf [15] recently confirmed that the CO_2 partial pressure affects the initial decomposition temperature of dolomite. Therefore, further investigations under more accurately controlled atmospheres will be necessary for Mg-kutnahorite.

Decomposition temperature of $CaCO_3$

Figure 12 shows the endothermic peaks due to the decomposition of $CaCO_3$ for Mg-kutnahorite, dolomite and mechanical mixtures of $CaCO_3$ and MnO_2 or $MnCO_3$. The curves (E) and (F) represent the second endothermic peaks of dolomite in CO_2 and in $CO_2 + CO$, which were caused by the decomposition of $CaCO_3$ formed by the partial decomposition of the original

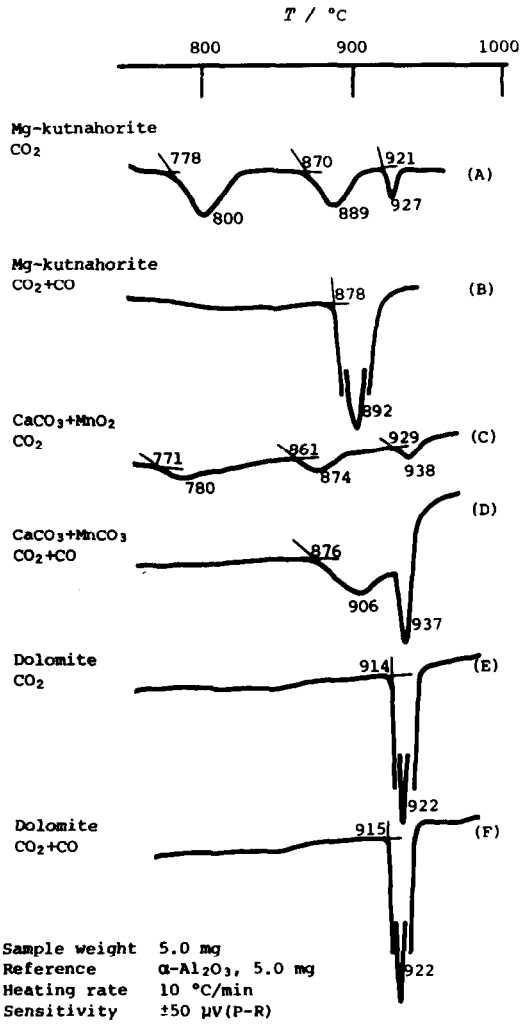

Fig. 12. The decomposition temperatures of $CaCO_3$ under various experimental conditions.

dolomite. They show that the small difference in CO_2 partial pressure in CO_2 and in CO_2 + CO hardly affects the temperature regions of the second peaks. The curves (A) and (B) show the endothermic peaks of Mg-kutnahorite related to the decomposition of $CaCO_3$ in CO_2 and in CO_2 + CO. Considering the results of dolomite just mentioned, it is suggested that the remarkable difference in temperature regions among the peaks of curves (A) and (B) reflects the difference in the reaction temperatures of $CaCO_3$ with coexisting Mn-compounds. In the curves (A) and (B), all peaks shift to lower temperatures except the last small peak of (A) in the same temperature region as the second peak of dolomite. In order to examine whether these temperature shifts are the characteristic features of the decomposition of Mg-kutnahorite,

two samples were prepared to be compared with the curves (A) and (B). One is the mechanical mixture of $CaCO_3$ (calcite) and MnO_2 (pyrolusite) with the mole ratio of 1 : 1, and the other is the mixture of $CaCO_3$ (calcite) and MnO with the mole ratio of 1 : 1. MnO was obtained by decomposition of $MnCO_3$ (rhodochrosite) in CO_2 + CO. Their DTA curves (C) and (D) were obtained in the same atmospheres as (A) and (B).

The curve (C) has two endothermic peaks corresponding to the first two peaks of (A). Compared with the third peak of the curve (A), that of (C) appears at a slightly higher temperature, reflecting the good crystallinity of calcite used in the preparation of the mixture.

The curve (D) shows the very broad endothermic peak in the same temperature region as the endothermic peak of (B), immediately followed by the sharp endotherm caused by the decomposition of the $CaCO_3$ which remained unreacted with the Mn-oxides.

These results clearly indicate that the low temperature decompositions related to $CaCO_3$ are not characteristic features for Mg-kutnahorite, but are commonly recognizable ones whenever $CaCO_3$ is heated with Mn-oxides. Therefore, after the destruction of its dolomite structure, Mg-kutnahorite is only a supplier of the mixtures of the very fine $CaCO_3$ and some Mn-compounds whose compositions are controlled by the atmospheres applied. These mixtures may be regarded as identical to the mechanical mixtures of the component materials.

CONCLUSIONS

From these results, the thermal decomposition of kutnahorite may be described generally as follows.

In the CO_2 partial pressure at which dolomite shows two widely separated endothermic peaks, kutnahorite decomposes through two completely different processes depending on the O_2 partial pressure of the atmosphere.

If the O_2 partial pressure is so low that Mn remains bivalent, kutnahorite decomposes in two steps like dolomite. At the first step, $CaCO_3$ and periclase type solid solution are produced releasing the corresponding amount of CO_2 to Mn and Mg. At the second step, lime type solid solution is formed by the decomposition of $CaCO_3$. At this step, the equilibrium redistribution of Mn between periclase and lime type solid solutions is achieved due to the thermodynamic stabilization.

If the O_2 partial pressure is so high that Mn is oxidized, at the first step, $CaCO_3$ and one or more Mn-Mg-oxides, whose compositions are determined by the oxidation state of Mn and the ratio of Mn to Mg, are produced. On further heating, the Mn-Mg-oxides expel MgO as a single phase and the resultant Mn-oxides produce some Ca-Mn-oxides, such as $CaMnO_3$ and Ca_2MnO_4, consuming $CaCO_3$ step by step. The greater the complexity of

these processes, the more complex is the corresponding DTA curve.

Kutnahorite, having the chemical composition of Ca/Mn of about 2, which was used as Mg-kutnahorite in this study, gives Ca_2MnO_4 as the final product. In addition, in the case of kutnahorite having a lower Ca/Mn ratio than Mg-kutnahorite, $Ca_4Mn_3O_{10}$, instead of Ca_2MnO_4, is obtained, as suggested by Shibuya and Harada [4].

As the chemical compositions of the final products strongly depend on that of the original material, the detailed examination of the chemical composition of the sample is most important in the study of the decomposition of the carbonate of dolomite-kutnahorite series.

ACKNOWLEDGEMENTS

We thank Mr. H. Tatematsu, Railway Technical Research Institute, JNR, for permission to use the high-power X-ray diffractometer and Dr. Y. Ogasawara and Mr. N. Tomioka, Waseda University, for help with EPMA analysis.

This study was partly supported by the Grant in Aid for the Scientific Research of the Ministry of Education, Japan (C-56550447).

REFERENCES

1 C. Frondel and L.H. Bauer, Am. Mineral., 40 (1955) 748.
2 D.N. Todor, Thermal Analysis of Minerals, Abacus Press, Tunbridge Wells, 1976, p. 180.
3 A. Tsusue, Am. Mineral., 52 (1967) 1751.
4 G. Shibuya and S. Harada, J. Mineral. Soc. Jpn., 13 (1976) 1.
5 R. Otsuka, S. Tanabe and K. Iwafuchi, J. Mineral. Metall. Inst. Jpn., 96 (1980) 581.
6 R. Otsuka, S. Tanabe, K. Iwafuchi and R. Ozao, Proc. 6th Int. Conf. Therm. Anal., Bayreuth, Vol. 2, 1980, p. 295.
7 K. Tanida, T. Kitamura and M. Nambu, J. Jpn. Assoc. Mineral. Petrol. Econ. Geol., 76 (1981) 32.
8 P.V. Riboud and A. Muan, J. Am. Ceram. Soc., 46 (1963) 33.
9 R.C. Doman, J.B. Barr, R.N. McNally and A.M. Alper, J. Am. Ceram. Soc., 46 (1963) 313.
10 A.H. Jay and K.W. Andrews, J. Iron and Steel Inst., London, 152 (1945) 15.
11 W.C. Hahn, Jr. and A. Muan, Mater. Res. Bull., 5 (1970) 955.
12 N. Tiberg and A. Muan, Metall. Trans., 1 (1970) 435.
13 R.A. Robie and D.R. Waldbaum, U.S. Geol. Surv. Bull., 1259 (1968).
14 R.A.W. Haul and H. Heystek, Am. Mineral., 37 (1952) 166.
15 W.R. Bandi and G. Krapf, Thermochim. Acta, 14 (1976) 221.